Field-Induced Orbital and Magnetic Phases in $Ca_3Ru_2O_7$

J. F. Karpus, R. Gupta, H. Barath, and S. L. Cooper*

Department of Physics and Frederick Seitz Materials Research Laboratory, University of Illinois at Urbana-Champaign, Urbana, Illinois 61801 USA

G. Cao

Department of Physics and Astronomy, University of Kentucky, Lexington, Kentucky 40506 USA

(Received 7 June 2004; published 14 October 2004)

Magnetic-field- and temperature-dependent Raman scattering studies of $Ca_3Ru_2O_7$ reveal dramatic field-dependent properties arising from transitions between various complex orbital and magnetic phases, including a field-induced orbital-ordered to orbital-disordered transition ($H_o\|$ hard axis), and a reentrant orbital-ordered to orbital-disordered to orbital-ordered transition ($H_o\|$ easy axis). We find that the dramatic magnetic-field properties are most prevalent in a "mixed"-magnetic and -orbital phase regime, providing evidence for a strong connection between orbital phase inhomogeneity and "colossal" field effects in the ruthenates.

DOI: 10.1103/PhysRevLett.93.167205 PACS numbers: 75.25.+z, 71.30.+h, 78.30.–j

Many of the exotic phases and phenomena exhibited by transition metal oxides (TMO) reflect the importance of the orbital degree of freedom, which interacts strongly with the spins, charges, and lattice via Jahn-Teller, spin-orbit, and other interactions [1]. In $La_{1-x}(Sr, Ca)_xMnO_3$, for example, partial filling of the e_g orbitals leads to a splitting of degenerate $d(e_g)$ states via a cooperative Jahn-Teller distortion of the MnO_6 octahedra, contributing to such phenomena as orbital ordering, polaron formation, and electronic phase separation [1,2]. Although less thoroughly studied, TMO with partially filled t_{2g} orbitals, such as the titanates, vanadates, and ruthenates, are potentially more rich and interesting, due to both the higher degeneracy of the t_{2g} states and the strong spin-orbit interaction in these TMO. The exotic orbital physics associated with these TMO includes coherent orbital-liquid phases in YVO_3 and $LaTiO_3$, [3,4] orbital ordering phases in the vanadates [5] and ruthenates [6,7], and "orbital selective" Mott transitions [7,8].

The layered ruthenates $(Sr, Ca)_{n+1}Ru_nO_{3n+1}$ (n = number of Ru-O layers/unit cell) [9] have been of particular interest recently because of their diversity of doping-induced phases, from orbital-ordered Mott insulator in Ca_2RuO_4 [7,9] and $Ca_3Ru_2O_7$ [9] to exotic superconductor in Sr_2RuO_4 [9] or exotic metal in $Sr_3Ru_2O_7$ [10]. However, the ruthenates are also characterized by a wealth of magnetic-field-induced phases [10,11], due to strong spin-orbit coupling in the $4d$ shell of Ru [12]. The ruthenates also exhibit rich orbital physics, such as a strong dependence of the orbital population on temperature and pressure in Ca_2RuO_4 [12–14] and $Ca_3Ru_2O_7$ [15,16], and evidence for a "d_{xy}" orbital-ordered ground state consisting of an approximate hole distribution of 0.5 and 1.5 on the d_{xy} and $d_{yz/zx}$ orbitals in Ca_2RuO_4 [12].

This Letter describes an inelastic light (Raman) scattering study of the magnetic-field-induced orbital and magnetic phases in $Ca_3Ru_2O_7$ ($T_N = 56$ K; $T_{MI} = 48$ K). In contrast to transport and magnetic measurements [11], this study allows us to directly probe the field-induced evolution of the orbital configuration, as well as the attendant changes of the spin dynamics and structural properties, in $Ca_3Ru_2O_7$. Our investigation reveals a rich orbital and magnetic phase diagram in $Ca_3Ru_2O_7$, which is precipitated by the interplay between applied field, magnetic exchange, and spin-orbit coupling.

Raman scattering measurements were performed on $Ca_3Ru_2O_7$ single crystals at temperatures 11.5–300 K, and in magnetic fields up to 9 T. Spectra were obtained with the applied field (H_o) parallel to both the (easy) a axis ($[1, 1, 0]$) and (hard) b axis ($[1, -1, 0]$), with the incident and scattered photon wave vectors $\mathbf{q} \perp H_o$ (Voigt geometry), and with circular polarized incident and scattered photon polarizations. Figures 1(a)–1(d) show representative field-dependent Raman spectra of $Ca_3Ru_2O_7$ with $H_o\|a$ axis, illustrating the two key spectroscopic features with which we are able to explore the

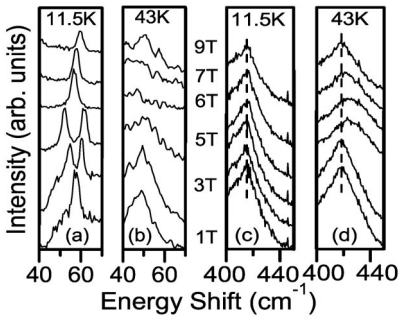

FIG. 1. Representative magnon and phonon Raman intensities for $Ca_3Ru_2O_7$ as a function of magnetic-field ($H_o\|a$ axis): 57 cm^{-1} magnon spectrum at (a) $T = 11.5$ K and (b) $T = 43$ K ($\times 3.8$), and Ru-O out-of-phase c-axis phonon spectrum at (c) $T = 11.5$ K and (d) $T = 43$ K ($\times 0.84$).

 0031-9007/04/93(16)/167205(4)$22.50

field-induced spin and orbital configurations in this material:

Spin configuration.—Figures 1(a) and 1(b) show a low-frequency mode near 57 cm^{-1} associated with spin wave (magnon) excitations of the antiferromagnetic (AF) ground state [15,16]. This mode was tentatively identified in zero-field Raman measurements [15] as a two-magnon (double spin flip, $\Delta S = 0$) excitation, based on the mode's temperature dependence and symmetry. However, the magnetic-field-induced splitting observed in this study allows us to more conclusively identify the 57 cm^{-1} mode as a single-magnon (single spin flip, $\Delta S = \pm 1$) excitation. Here, we use this magnon to monitor the field dependent spin configuration in $Ca_3Ru_2O_7$.

Orbital configuration.—Figures 1(c) and 1(d) show the field dependence of the Ru-O phonon near 416 cm^{-1} in $Ca_3Ru_2O_7$. This mode is exquisitely sensitive to the RuO_6 octahedral structure and orbital population as functions of temperature [15] and pressure [16]: it has an energy $\sim$433 cm^{-1} in the *metallic* [11] orbital-degenerate phase ($T > T_{MI} = 48$ K), in which regime the RuO_6 octahedra are undistorted ($d_{\perp}^{RuO} \sim d_{\parallel}^{RuO}$; $d_{\perp}^{RuO}$and $d_{\parallel}^{RuO}$ = apical and in-plane Ru-O bond lengths) and the four Ru d electrons have an approximate d-orbital distribution $(n_{yz/zx}, n_{xy}) \sim (8/3, 4/3)$ [7]. However, this mode softens dramatically to less than $\sim$418 cm^{-1} in the *insulating* [11] "d_{xy}" orbital-ordered (OO) phase of $Ca_3Ru_2O_7$. In this phase, the RuO_6 octahedra become compressed ($d_{\perp}^{RuO} < d_{\parallel}^{RuO}$) [17], which lowers the energy of the d_{xy} orbitals relative to that of the $d_{yz/zx}$ orbitals, and causes an approximate d-orbital distribution of $(n_{yz/zx}, n_{xy}) \sim (2, 2)$ [18]. Here, we exploit the strong correlation of this Ru-O phonon energy with orbital distribution to investigate *field-induced* changes in $d_{\perp}^{RuO}/d_{\parallel}^{RuO}$ and the orbital configuration.

For fields $H_o||a$ axis (= [1, 1, 0]), the field-dependent spectra summarized in Figs. 2(a)–2(c) reveal several interesting field-induced magnetic and orbital phases:

(i) *Orbital-degenerate regime.*—For $T > T_{MI}$(= 48 K) and in moderate fields ($H_o < H^*$), the Ru-O phonon energy is roughly 433 cm^{-1}, suggesting that the Ru ions have an approximate d-orbital population $(n_{yz/zx}, n_{xy}) = (8/3, 4/3)$ and that the RuO_6 octahedra are undistorted, $d_{\perp}^{RuO} \sim d_{\parallel}^{RuO}$. Interestingly, although transport and magnetic measurements suggest that this regime ($T_{MI} < T < T_N$) is an AF *metal* with moments oriented along the b axis [11], no magnon response is observed, presumably because it is overdamped by itinerant charges.

(ii) *AF/OO regime.*—At low temperatures ($T \ll T_N$) and applied fields, $H_o < H_c$, the magnon mode near 57 cm^{-1} is clearly observed and splits into two modes with increasing field. This field-dependent splitting is consistent with the behavior expected of $\mathbf{k} = 0$ spin waves in a simple two-sublattice AF ($H_o||$ easy axis), which have energies given by

$$\omega^{\pm}(\mathbf{k} = 0) \cong [\alpha J_{\perp}(\mathbf{k} = 0) + \beta J_{||}(\mathbf{k} = 0) + g\mu_B H_A] \pm g\mu_B H_o = \Delta^{AF} \pm g\mu_B H_o,$$

where $J_{\perp}(\mathbf{k} = 0)$ and $J_{||}(\mathbf{k} = 0)(\sim g\mu_B H_E)$ are the interlayer and intralayer exchange coupling parameters, H_A and H_E are the in-plane anisotropy and exchange fields, and α and β are exchange parameters [19]. In the case of A-type AF $Ca_3Ru_2O_7$ [in-plane ferromagnetic (FM), interplane AF] [11], the spin waves associated with these two energies can be attributed to spins precessing in opposite senses on adjacent Ru-O layers. The observed splitting of the magnon energies at $H_o = 5$ T and $T = 11.5$ K is $\Delta\omega^{\pm} = 9.5$ cm^{-1} [Fig. 2(a)], which is consistent with $2g\mu_B H_o = 9.3$ cm^{-1} for $g = 2$. Also, the large magnon energy reflects a substantial AF spin gap $\omega^{\pm}(H_o = 0) = \Delta^{AF} = 57$ cm^{-1}, indicative of the large exchange and anisotropy fields in $Ca_3Ru_2O_7$. Significantly, throughout the AF-OO temperature and field re-

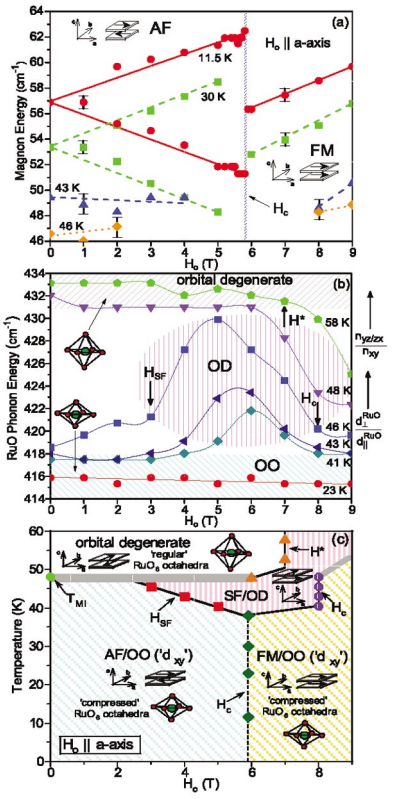

FIG. 2 (color). (a) Magnon energy vs magnetic-field for various temperatures in $Ca_3Ru_2O_7$ with $H_o||a$ axis. (b) Ru-O phonon energy vs magnetic field for various temperatures with $H_o||a$ axis, illustrating OO and OD regimes. (c) H_o-T phase diagram for $H_o||a$ axis, deduced from results in (a) and (b). Squares denote transition between AF/OO and SF/OD phases, diamonds denote transition between AF/OO and FM/OO phases, purple circles denote transition between SF/OD and FM/OO phases, and triangles denote transition between orbital-degenerate and SF/OD phases.

gime, the Ru-O phonon mode is field independent and has a low-frequency value ≤ 418 cm^{-1}, indicating that orbital ordering persists in this phase. Indeed, transport measurements indicate insulating behavior in this regime [11], presumably due to the weak hybridization associated with the occupied d_{xy} orbitals [7,8].

(iii) *FM/OO regime.*—As shown in Fig. 2, for $H_o > H_c \sim 5.9$ T, the split AF magnon modes collapse to a single-magnon mode, indicating a *metamagnetic transition* from an A-type AF configuration to a FM configuration. Metamagnetic transitions are expected for $H_o = H_c$ ($= 2H_E - H_A$ [19]) when a material's anisotropy field H_A is larger than its exchange field H_E [20]. Hysteretic behavior between Raman spectra obtained when increasing and decreasing the field confirm that the metamagnetic transition is first order. Importantly, Fig. 2(b) shows that the Ru-O phonon mode maintains its "low" OO value through the metamagnetic transition in $Ca_3Ru_2O_7$, indicating that neither the orbital configuration nor the RuO_6 octahedral structure are influenced by this transition. This is consistent with the fact that the moments remain oriented along the easy-axis direction through this transition, and therefore induce no orbital rearrangement via the spin-orbit interaction.

Several important $T \sim 0$ parameters can be extracted from the magnon spectra measured well below T_N (at $T = 11.5$ K). For $H_o > H_c$ and $J_\perp \ll J_\parallel$, the field-dependent FM magnon energy is given by

$$\omega^{\mathrm{FM}} \cong [g\mu_B H_E - \alpha J_\perp + g\mu_B H_A] + g\mu_B H_o,$$

[19], which is consistent with the measured field dependence, $\Delta E/\Delta H_o \sim 1$ cm$^{-1}/T$, of the magnon energy in Fig. 2(a). From the observed critical field H_c in $Ca_3Ru_2O_7$, we can estimate an interlayer exchange energy of $g\mu_B H_c = \alpha J_\perp \sim 5.5$ cm^{-1} (0.7 meV). Note also that the linear extrapolation of ω^{FM} (H_o) back to zero field (i.e., FM spin gap) in the FM-OO regime is $\Delta^{\mathrm{FM}} \sim 49.5$ cm^{-1}, which is roughly 7.5 cm^{-1} lower than the measured AF spin-gap energy $\Delta^{\mathrm{AF}} \sim 57$ cm^{-1}. The difference between the zero-field AF and FM magnon energies is expected to be $\Delta\omega \sim 2\alpha J_\perp = 2g\mu_B H_c = 11$ cm^{-1}, which compares reasonably with the measured difference, $\Delta\omega \sim 8$ cm^{-1} (1 meV) in Fig. 2(a). Finally, from the critical field energy $g\mu_B H_c (= \alpha J_\perp) \sim 5.5$ cm^{-1}, the AF spin-gap $\Delta^{\mathrm{AF}} \sim 57$ cm^{-1}, and the relationship $H_c = 2H_E - H_A$ [20], we estimate $H_A \sim 35$ T in $Ca_3Ru_2O_7$ at $T = 11.5$ K. These values are somewhat larger than estimates obtained from the low-T magnetic susceptibility, $H_A \sim 22.4$ T and $H_E \sim 14.2$ T [11]. Figure 2(a) shows, however, that Δ^{AF} and Δ^{FM} decrease with increasing T, indicating that H_A, H_E, and H_A/H_E systematically decrease with increasing T in $Ca_3Ru_2O_7$. Note that the temperature dependences of Δ^{AF} and Δ^{FM} are consistent with magnon frequency renormalization predicted by spin wave theory and with the temperature-dependent magnon energies experimentally observed in other AF and FM systems [19].

(iv) *SF/OD regime.*—In contrast to the metamagnetic transition in $Ca_3Ru_2O_7$, which has no influence on the orbital population, Fig. 2(b) shows that the Ru-O phonon frequency at higher temperatures ($30\,\mathrm{K} < T < T_N$) increases rapidly with increasing field, then subsequently decreases with field back to its zero-field value. This field-induced phonon energy renormalization reflects an evolution of the orbital configuration in $Ca_3Ru_2O_7$ from an AF "d_{xy}"-OO arrangement $(n_{yz/zx}, n_{xy}) = (2, 2)$ for $H_o < H_{\mathrm{SF}}$ to an "orbital-disordered" (OD) configuration ($H_{\mathrm{SF}} < H_o < H_c$) in which the RuO_6 octahedral structure and Ru d-orbital population first change rapidly with field toward their orbital-degenerate values, $d_\perp^{\mathrm{RuO}} \sim d_\parallel^{\mathrm{RuO}}$ and $(n_{yz/zx}, n_{xy}) \sim (8/3, 4/3)$, then return rapidly to their OO configurations at higher fields. At still higher fields, $H_o > H_c$, the Ru-O phonon frequency saturates at its low-frequency, OO value, and a weak FM magnon reappears [Fig. 1(a)], revealing a transition to a "reentrant" d_{xy}-OO (FM) phase when H_o ($\|a$ axis) is large enough to align the moments along the a axis.

This complex and interesting field-tuned behavior of the orbital distribution is clearly associated with the appearance of a "spin-flop" (SF) phase at intermediate fields and temperatures in $Ca_3Ru_2O_7$ [Fig. 2(c)]. In contrast with a metamagnetic transition, an antiferromagnet with $H_A < H_E$ is expected to evolve with field from AF to FM phases ($H_o > H_c$) *through* an intermediate SF phase for $H_{\mathrm{SF}} < H_o < H_c$. In this phase, the moments align roughly *transverse* to the applied field before gradually aligning themselves with the applied field for $H_o > H_c$ [20]. In systems with strong spin-orbit coupling, such as $Ca_3Ru_2O_7$, this "flopping" of some fraction of the moments from the (easy) a-axis to the (hard) b-axis in the SF phase naturally results in a field-dependent reorganization of orbital populations on the affected sites. Importantly, several features in the data, including the gradual reduction of magnon intensity in the SF-OD regime [Fig. 1(a)], the rather broad field region over which the Ru-O phonon frequency is observed to change [Fig. 2(b)], and the field-hysteretic behavior observed in the Raman spectra, all suggest that this interesting SF phase is both magnetically and orbitally disordered, consisting of a random mixture of a- and b-axis oriented moments and orbital populations on different Ru sites or Ru-O layers. Evidence for "mixed-phase" behavior in the SF-OD regime of $Ca_3Ru_2O_7$ is particularly noteworthy in view of the large magnetoresistance observed in this regime [11], as it suggests that the intimate connection between mixed-phase behavior and "colossal" field and pressure effects established in the manganese perovskites [2] extends also to the layered ruthenates.

The field-induced phases revealed by the Raman spectra for $H_o \| b$ axis [Figs. 3(a) and 3(b)] are much simpler

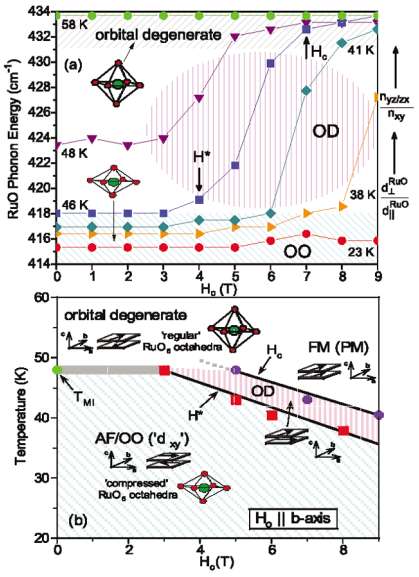

FIG. 3 (color). (a) Ru-O phonon energy vs magnetic field for various temperatures in $Ca_3Ru_2O_7$ with $H_o||b$ axis, illustrating OO and OD phases. (b) H_o-T phase diagram with $H_o||b$ axis. Squares denote transition between AF/OO and OD phases and purple circles denote transition between SF/OD and FM/OO phases.

than for $H_o||a$ axis: with increasing H_o ($||b$ axis), there is a systematic increase of the Ru-O phonon energy [Fig. 3(a)], and a concomitant diminution of the magnon intensity. This is indicative of a field-tuned "quantum melting" transition from the AF d_{xy}-OO phase $[(n_{yz/zx}, n_{xy}) \sim (2, 2)]$ for $H_o < H^*$, in which the applied field is insufficient to reorient the moments away from the (easy) a axis, to the high-field *FM orbital-degenerate* regime $[(n_{yz/zx}, n_{xy}) \sim (8/3, 4/3)]$ for $H_o > H_c$, in which the applied field is of sufficient strength to orient most of the moments along the b axis. Most interesting is the intermediate-field and -temperature OD regime, $H^* < H_o < H_c$, which is characterized by a rapid increase in the Ru-O phonon energy with field [Fig. 3(a)], and hence a rapid increase in both $n_{yz/zx}/n_{xy}$ and $d_\perp^{\mathrm{RuO}}/d_\parallel^{\mathrm{RuO}}$ with field. Substantial evidence suggests that this phase regime is orbitally disordered and composed of a mixture of a- and b-axis oriented moments, and is therefore akin to the SF-OD regime observed for $H_o||a$ axis: the magnon intensity decreases systematically with field, the spectra exhibit hysteretic behavior, and the Ru-O phonon energy is strongly field dependent over a broad field range. Significantly, this OD phase regime also exhibits the most dramatic magnetoresistance when $H_o||b$ axis [11].

These spectroscopic results demonstrate that the dramatic field-induced transport properties in $Ca_3Ru_2O_7$ [11] are spawned by large field-induced orbital and structural changes made possible by the strong spin-orbit coupling in the 4d shell of Ru. Additionally, this study demonstrates the very different electrical and magnetic properties associated with different orbital configurations in $Ca_3Ru_2O_7$, specifically between the insulating d_{xy} OO configuration, which has a compressed RuO_6 structure, moments oriented $||a$ axis, and well-defined magnons in the Raman spectra, and the metallic orbital-degenerate configuration, which has a "regular" RuO_6 structure, moments $||b$ axis, and no evidence for magnons. This disparate behavior reflects substantial differences in the degree to which different Ru (d) orbitals hybridize between neighboring sites.

We acknowledge useful discussions with E. Dagotto and M.V. Klein and support of this work by the National Science Foundation Under Grants No. DMR02-44502 (S. L. C.) and No. DMR02-40813 (G. C.), the Department of Energy under Grant No. DEFG02-91ER45439 (S. L. C.), and the Sony Corporation.

*Corresponding author: s_cooper@mrl.uiuc.edu

[1] Y. Tokura and N. Nagaosa, Science **288**, 462 (2000).
[2] For reviews, see M. B. Salamon and M. Jaime, Rev. Mod. Phys. **73**, 583 (2001); E. Dagotto, *Nanoscale Phase Separation and Colossal Magnetoresistance* (Springer, Berlin, 2003).
[3] G. Khaliullin, P. Horsch, and A. M. Oles, Phys. Rev. Lett. **86**, 3879 (2001); P. Horsch, G. Khaliullin, and A. M. Oles, Phys. Rev. Lett. **91**, 257203 (2003).
[4] G. Khaliullin, Phys. Rev. B **64**, 212405 (2001).
[5] H. F. Pen *et al.*, Phys. Rev. Lett. **78**, 1323 (1997); F. Mila *et al.*, Phys. Rev. Lett. **85**, 1714 (2000).
[6] T. Hotta and E. Dagotto, Phys. Rev. Lett. **88**, 017201 (2001).
[7] V. I. Anisimov *et al.*, Eur. Phys. J. B **25**, 191 (2002).
[8] A. Koga *et al.*, Phys. Rev. Lett. **92**, 216402 (2004).
[9] S. Nakatsuji and Y. Maeno, Phys. Rev. B **62**, 6458 (2000); G. Cao *et al.*, Phys. Rev. B **56**, 5387 (1997).
[10] R. S. Perry *et al.*, Phys. Rev. Lett. **92**, 166602 (2004).
[11] G. Cao *et al.*, Phys. Rev. B **69**, 014404 (2004); S. McCall, G. Cao, and J. E. Crow, Phys. Rev. B **67**, 094427 (2003).
[12] T. Mizokawa *et al.*, Phys. Rev. Lett. **87**, 077202 (2001).
[13] J. S. Lee *et al.*, Phys. Rev. Lett. **89**, 257402 (2002); J. H. Jung *et al.*, Phys. Rev. Lett. **91**, 056403 (2003).
[14] F. Nakamura *et al.*, Phys. Rev. B **65**, 220402 (2002).
[15] H. L. Liu *et al.*, Phys. Rev. B **60**, R6980 (1999).
[16] C. S. Snow *et al.*, Phys. Rev. Lett. **89**, 226401 (2002).
[17] M. Braden *et al.*, Phys. Rev. B **58**, 847 (1998).
[18] In this Letter we assume that the OO configuration involves a ferro-orbital ordering configuration [7,13], although we are not able to rule out an antiferro-orbital ordering arrangement [6] from our Raman spectra.
[19] M. G. Cottam and D. J. Lockwood, *Light Scattering in Magnetic Solids* (John Wiley & Sons, New York, 1986).
[20] L. J. D. Jongh and A. R. Meidema, Adv. Phys. **50**, 947 (2001).